

Synthesis of Direct β -to- β Linked Porphyrin Arrays with Large Electronic Interactions: Branched and Cyclic Oligomers**

Hao Cai, Keisuke Fujimoto, Jong Min Lim, Chaojie Wang, Weiming Huang, Yutao Rao, Senmiao Zhang, Hui Shi, Bangshao Yin, Bo Chen, Ming Ma, Jianxin Song,* Dongho Kim,* and Atsuhiko Osuka*

Abstract: Direct β -to- β linked branched and cyclic porphyrin trimers and pentamers have been synthesized by the Suzuki–Miyaura coupling of β -borylporphyrins and β -bromoporphyrins. The cyclic porphyrin trimer, the smallest directly linked cyclic porphyrin wheel to date, and its twined pentamer, exhibit small electrochemical HOMO–LUMO gaps, broad nonsplit Soret bands, and red-shifted Q-bands, thus indicating large electronic interactions between the constituent porphyrin units.

Cyclic porphyrin arrays have been extensively explored as synthetic models of photosynthetic antennae and functional hosts possessing convergent multidentate coordination sites.^[1–4] Cyclic porphyrin structures are usually ensured by employing appropriately bent bridges or assisted by a tilting distortion of the porphyrins and/or bridges. Efficient excitation-energy “hopping” along the cyclic array is enhanced by the close proximity of porphyrins or conjugated spacers, both of which increase the electronic communication between constituent porphyrins. As a rare and extreme case, directly meso-to-meso linked cyclic porphyrin arrays (without a spacer) have been explored as photosynthetic models using a 5,10-diaryl zinc(II) porphyrin building block.^[5] While these porphyrin rings display efficient excitation-energy transfer, they are rather nonconjugative owing to the tilted conformations of the porphyrin constituents, a feature inherent to meso-to-meso linked porphyrin arrays.^[6] Herein, we report the synthesis of a direct β -to- β linked porphyrin trimer, the smallest directly linked porphyrin wheel known to date, and its twined pentamer. These porphyrin oligomers display large electronic interactions among the constitutional porphyrins owing to less tilted structures.

We found that treatment of the β -borylated porphyrins **2** and **3** (Figure 1), which were prepared by iridium-catalyzed β -selective borylation of the 5,10,15-triaryl nickel(II) porphyrin **1**,^[7] with CuBr_2 in THF at 105 °C overnight^[8] gave the β -bromoporphyrins **4** and **5** in 80 and 85 % yield, respectively. Suzuki–Miyaura coupling of **2** with **4** in the presence of a $[\text{Pd}_2(\text{dba})_3]/\text{PPh}_3$ catalyst and cesium bases gave the direct β -to- β linked dimer **6** in 90 % yield. High yield of **6** can be ascribed partly to small steric constraints stemming from the absence of a meso substituent in **2** and **4**. This beneficial structural motif has been amply utilized in the synthesis of the U-shaped trimer **10**(Ni), from **2** and the dibromide **5**, in 50 % yield and the branched star-shaped pentamer **11**(Ni) from **4** and **7** in 35 %. The structures of **10**(Ni) and **11**(Ni) are fully consistent with their spectroscopic data (see the Supporting Information).

We also found that iridium-catalyzed borylation of **6** under standard reaction conditions furnished the diborylated linear nickel(II) porphyrin dimer **8** almost quantitatively in a highly regioselective manner. Then, we examined the Suzuki–Miyaura coupling of **8** and **5** with an expectation for the formation of cyclic porphyrin oligomers owing to the meso-free structural motif. To our delight, this was indeed true, in that cyclization proceeded smoothly to produce a directly linked cyclic porphyrin trimer, **12**(Ni), in 42 % yield, despite the predicted ring strain. High-resolution MALDI-TOF mass measurement detected the parent ion peak of **12**(Ni) at $m/z = 2789.49$ (calcd for $(\text{C}_{186}\text{H}_{210}\text{N}_{12}\text{Ni}_3)^+ = 2789.49$ ($[M]^+$)). The ^1H NMR spectrum of **12**(Ni) is quite simple, thus exhibiting only a single set of signals for the porphyrin and is in line with its symmetric structure. A singlet resulting from

[*] H. Cai, C. Wang, W. Huang, Y. Rao, S. Zhang, H. Shi, Dr. B. Yin, Prof. Dr. B. Chen, Prof. Dr. M. Ma, Prof. Dr. J. Song
Key Laboratory of Chemical Biology and Traditional Chinese
Medicine Research (Ministry of Education of China)
Hunan Normal University, Changsha 410081 (China)
E-mail: jxsong@hotmail.com

K. Fujimoto, Prof. Dr. A. Osuka
Department of Chemistry, Graduate School of Science
Kyoto University, Sakyo-ku, Kyoto 606-8502 (Japan)
E-mail: osuka@kuchem.kyoto-u.ac.jp

Dr. J. M. Lim, Prof. Dr. D. Kim
Spectroscopy Laboratory for Functional π -Electronic Systems
and Department of Chemistry, Yonsei University, Seoul 120-749
(Korea)
E-mail: dongho@yonsei.ac.kr

[**] We thank Prof. Xiaoyi Yi, Central South University (China) and Prof. Naoki Aratani, Nara Institute of Science and Technology (Japan), for

the determination and analysis of the X-ray Structure. The work at Hunan Normal University was supported by the National Natural Science Foundation of China. (Grant No. 21272065), the Aid Program for Science Innovative Research Team in Higher Educational institutions of Hunan Province, the Scientific Research Foundation for the Returned Overseas Chinese Scholars, State Education Ministry, and Scientific Research Fund of Hunan Provincial Education Department (Grant No.13k027). The work at Kyoto was supported by Grant-in-Aid from MEXT (Nos.: 25220802 (Scientific Research (S))). The work at Yonsei was supported by Global Research Laboratory (2013K1A1A2A02050183) and Global Frontier R&D Program on Center for Multiscale Energy System (2012-8-2081) funded by the National Research Foundation under the Ministry of Science, ICT & Future, Korea.



Supporting information for this article is available on the WWW under <http://dx.doi.org/10.1002/anie.201407032>.

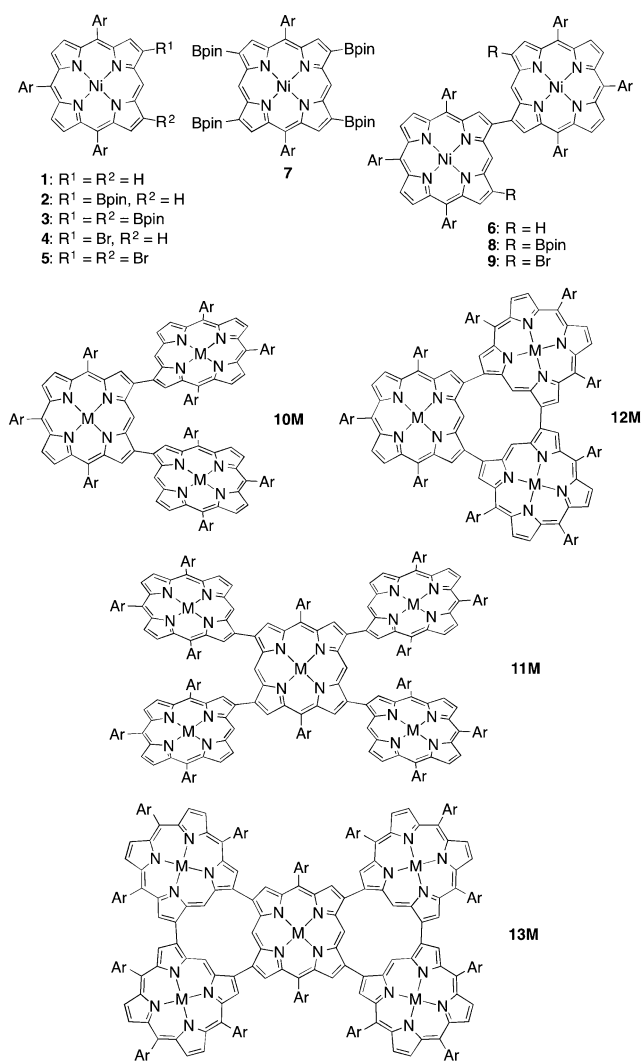


Figure 1. Porphyrin compounds studied in this paper. Ar = 3,5-di-*tert*-butylphenyl, Bpin = pinacolatoboryl, M = metal.

the meso proton was observed at $\delta = 12.41$ ppm. Then, the dimer **8** was converted into the β,β' -dibrominated porphyrin dimer **9** in 80 % yield under the above-mentioned bromination conditions. This dimer was coupled with **3** through the Suzuki–Miyaura reaction to give the same trimer **12**(Ni) in a comparable yield of 40 %. Finally, the coupling of **7** with 2 equivalents of **9** provided the porphyrin pentamer **13**(Ni), which possesses a twined cyclic trimeric structure, in 20 % yield. The parent ion peak of **13**(Ni) was observed at $m/z = 4458.32$ (calcd for $(C_{296}H_{328}N_{20}Ni_5)^+ = 4458.31$ ($[M]^+$) in the high-resolution MALDI-TOF mass spectrum, and the 1H NMR spectrum displayed two meso-proton singlets at $\delta = 12.28$ and 12.02 ppm in a ratio of 2:1, which is consistent with the twined structure (see the Supporting Information).

Definitive structural confirmation of **13**(Ni) was provided by X-ray diffraction analysis, which revealed a twined cyclic trimeric structure (Figure 2).^[9] All of the porphyrin subunits are highly twisted and none of the porphyrin cores are coplanar with respect to each other. The maximum displacements of the β -carbon atoms from the porphyrin mean plane

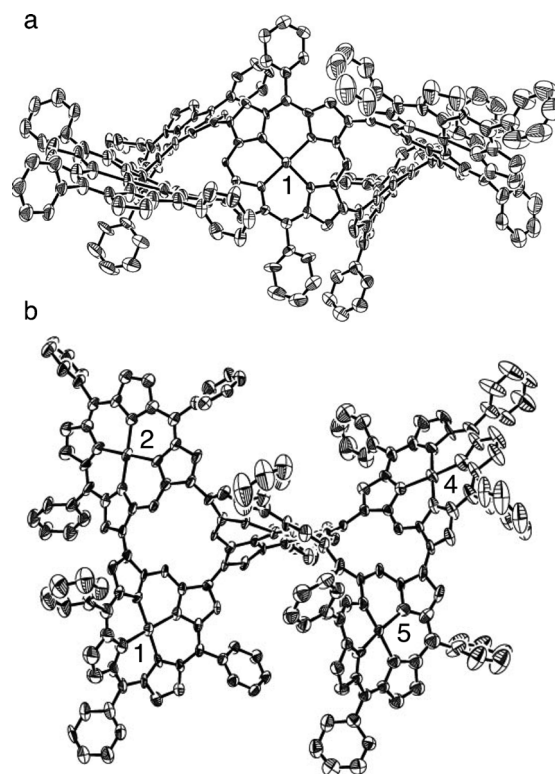


Figure 2. X-ray structure. a) Top view and b) side view of **13**(Ni). The thermal ellipsoids are 50 % probability level. *tert*-Butyl groups and hydrogen atoms are omitted for clarity.

are 1.289 Å for the central porphyrin and 0.744 Å on average for the peripheral porphyrins. The central porphyrin plane is highly tilted relative to the peripheral porphyrins with dihedral angles ranging from 66° to 71°, while the two peripheral porphyrins within the same cyclic trimer are more coplanar with small dihedral angles of 11° and 34°. This conformation means that the porphyrins in the cyclic trimeric ring are in a coplanar arrangement as a result of the strain associated with the ring structure.

The electrochemical properties of **1**, **6**, and **10**(Ni)–**13**(Ni) were investigated by cyclic voltammetry and differential pulse voltammetry (Table 1). The monomer **1** exhibits two oxidation potentials at 0.48 and 0.87 V and a reduction potential at -1.83 V, which leads to an electrochemical HOMO–LUMO gap (ΔE_{HL}) of 2.31 eV. The dimer **6** shows oxidation potentials at 0.47 and 0.62 V, which have been interpreted as split first potentials with $\Delta V_O = 0.15$ V owing to the electronic interaction of the two nickel(II) porphyrins.^[10] The ΔE_{HL} value for **6** is 2.35 eV. The branched oligomers **10**(Ni) and **11**(Ni) display more complicated electrochemical responses, that is, they show five oxidation potentials and two reduction potentials. Since these arrays contain different nickel(II) porphyrin units, comparison of ΔV_O is not easy but the ΔE_{HL} values of **10**(Ni) and **11**(Ni) are both 2.16 eV, and slightly smaller than those of **1** and **6**. Importantly, the symmetric cyclic trimer **12**(Ni) displays oxidation potentials at 0.34, 0.57, and 0.68 V and reduction potentials at -1.54 , -1.69 , and -1.90 V, which results in $\Delta E_{HL} = 1.88$ eV. The first two oxidation potentials of **12**(Ni) have been also interpreted

Table 1: Electrochemical properties of **1**, **6**, and **10(Ni)–13(Ni)** in CH₂Cl₂ with 0.1 M Bu₄NPF₆.^[a]

Compound	E_{ox5}	E_{ox4}	E_{ox3}	E_{ox2}	E_{ox1}	E_{red1}	E_{red2}	E_{red3}	E_{red4}	ΔE_{HL} [eV]
1	–	–	–	0.87	0.48	–1.83	–	–	–	2.31
6	–	–	1.08	0.62	0.47	–1.88	–	–	–	2.35
10(Ni)	0.99	0.85	0.66	0.56	0.42	–1.74	–1.85	–	–	2.16
11(Ni)	1.06	0.86	0.60	0.49	0.45	–1.71	–1.81	–	–	2.16
12(Ni)	–	–	0.68	0.57	0.34	–1.54	–1.69	–1.90	–	1.88
13(Ni)	0.92	0.83	0.62	0.52	0.29	–1.46	–1.59	–1.78	–1.94	1.75

[a] Potentials (V) were determined vs ferrocene/ferrocenium ion by differential pulse voltammetry. Working electrode: glassy carbon. Counter electrode: Pt wire. Reference electrode: Ag/AgClO₄. Cyclic voltammetry experiments indicated that most of the redox processes were reversible (for details, see the Supporting Information).

as split potentials, thus leading to evaluation of $\Delta V_{\text{O}} = 0.23$ V. These data indicate that the electronic interaction in **12(Ni)** is larger than that of **10(Ni)** and **11(Ni)** because of the enforced cyclic structure. The cyclic pentamer **13(Ni)** exhibits electrochemical properties similar to those of **12(Ni)**, again indicating larger electronic interactions.

In the next step, demetalation of **10(Ni)–13(Ni)** gave the corresponding **10(H₂)–13(H₂)** and subsequent zinc(II) metalation provided **10(Zn)–13(Zn)** almost quantitatively. All these zinc(II) complexes were fully characterized by spectroscopic methods (see the Supporting Information). Figure 3 displays the UV/Vis absorption and fluorescence spectra of **10(Zn)–13(Zn)** in dichloromethane. The linear oligomers **10(Zn)** and **11(Zn)** exhibit split Soret bands at $\lambda = 416$ and 435 nm, and at $\lambda = 416$ and 470 nm, respectively, thus reflecting the presence of two different transition dipole moments

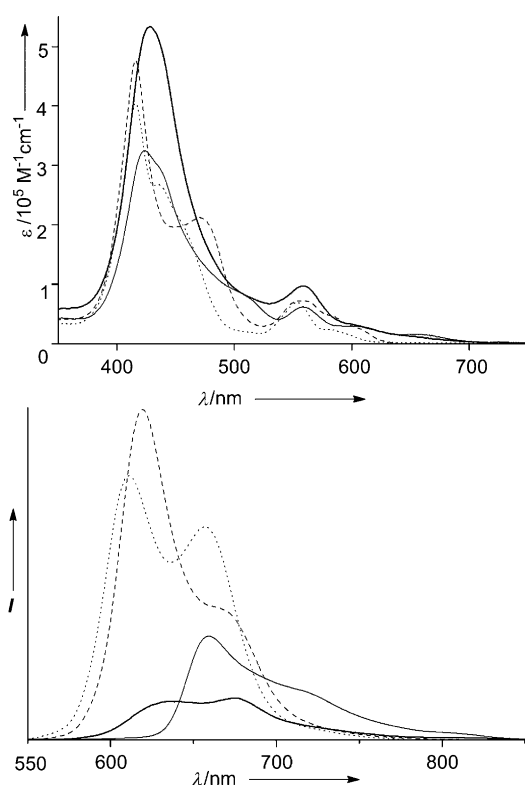


Figure 3. UV/Vis absorption (a) and fluorescence (b) spectra of **10(Zn)** (dotted line), **11(Zn)** (dashed line), **12(Zn)** (solid line), and **13(Zn)** (bold line) in CH₂Cl₂.

along the long molecular axis and short perpendicular axis. In contrast, the cyclic oligomers **12(Zn)** and **13(Zn)** both exhibit broader Soret and Q-bands which are presumably affected by large electronic interactions between the porphyrin units.^[5,11] The fluorescence spectra of **10(Zn)** and **11(Zn)** exhibit typical porphyrin-like vibronic structures with fluorescence quantum yields (Φ_{F}) of 0.033 and 0.056, respectively, while the fluorescence emission bands of **12(Zn)** and **13(Zn)** are red-shifted and the fluorescence quantum yields are considerably small, that is $\Phi_{\text{F}} = 0.013$ and 0.004, respectively. The fluorescence lifetimes of the noncyclic oligomers **10(Zn)** and **11(Zn)** were determined to be 2.1 nanoseconds, which is comparable to that of a zinc(II) porphyrin monomer (2.0 ns). However, the cyclic oligomers **12(Zn)** and **13(Zn)** revealed short fluorescence lifetimes of 800 and 560 picoseconds, respectively. While the fluorescence spectra of noncyclic oligomers are attributed to the monomeric porphyrin unit, the reduced fluorescence quantum yields and lifetimes of **12(Zn)** and **13(Zn)** may arise from large electronic interactions and structural strain associated with formation of the cyclic structure. Moreover, it should be noted that the previous direct β -to- β linked zinc(II) porphyrin dimer does not show the absorption features extending into NIR spectral region, and the fluorescence lifetime and quantum yield are 2.36 nanoseconds and 0.077, respectively.^[11] In this sense, the broad and structureless absorption spectra of the cyclic porphyrin oligomers, **12(Zn)** and **13(Zn)**, indicate large electronic interactions between the porphyrin units and may arise from not only their proximities but also coplanarity in the cyclic conformation.

The electronic interactions between the porphyrin units were investigated by femtosecond transient absorption (TA) spectroscopy (see the Supporting Information). Excitation-energy hopping processes along these cyclic or noncyclic porphyrin oligomers were investigated by Q-band excitations at $\lambda = 560$ nm with variable excitation power to avoid the involvement of S_2 - S_1 relaxation. Although the overall arrangement of energy hopping sites in the porphyrin oligomers may hamper precise estimation of energy hopping rates with a simple polygon model,^[5] it may provide fundamental insight into the exciton hopping processes in the porphyrin oligomers. In the cases of **6(Zn)**, **10(Zn)**, and **12(Zn)**, no distinctive power-dependent decay profiles were observed, probably because of the small number of porphyrin units and very fast internal exciton–exciton annihilation processes. However, the porphyrin pentamers **11(Zn)** and

13(Zn) displayed laser-power-dependent fast TA decays with time constants of 440 and 400 femtoseconds, respectively, most probably a result of efficient exciton–exciton annihilation processes (see the Supporting Information). To get more detailed information on the exciton hopping processes between the porphyrin units, transient absorption anisotropy (TAA) measurements were carried out (see the Supporting Information). With the very fast depolarization process (ca. 70 fs) originating from the equilibrium dynamics between the two degenerate transient dipoles in porphyrin monomer, additional depolarization processes were observed in the porphyrin oligomers. The anisotropy decay times were estimated to be about 170 and 250 femtoseconds for noncyclic porphyrin oligomers [**10**(Zn) and **11**(Zn)] and about 120 femtoseconds for the cyclic porphyrin trimer **12**(Zn). The estimated time constants are comparable to those observed in the direct meso-to-meso linked cyclic porphyrin arrays and are shorter than a β -to- β linked porphyrin dimer bridged by a saturated sp^3 -carbon atom, and shows an excitation-energy hopping time of 1.4 picoseconds.^[5,11] These features indicate that the excitation energy hopping processes occur efficiently in the directly linked porphyrin oligomers. Moreover, it should be noted that the cyclic porphyrin oligomers exhibit shorter time constants in exciton–exciton annihilation and anisotropy decay profiles than their linear congeners. In other words, strong electronic interactions between the porphyrin constituents are achieved in the cyclic porphyrin oligomers. Overall, the TAA and excitation-power-dependent TA experiments corroborate the acceleration of the exciton hopping time through the direct β -to- β direct linkages.

In summary, direct β -to- β linked cyclic porphyrin trimers and its twined pentamer were synthesized by Suzuki–Miyaura coupling of β -borylporphyrins and β -bromoporphyrins. The cyclic porphyrin oligomers exhibit optical and electrochemical properties different from those of the corresponding linear oligomers, properties such as nonsplit and broad Soret bands, red-shifted Q-bands, small electrochemical HOMO–LUMO band gaps, and reduced fluorescence quantum yields and lifetimes. Thus, the cyclic porphyrin trimers display efficient excitation-energy hopping along the ring. Further extension of this coupling strategy for the synthesis of more elaborate porphyrin arrays is actively in progress in our laboratories.

Received: July 9, 2014

Published online: August 25, 2014

Keywords: cross-coupling · cyclization · energy transfer · porphyrinoids · structure elucidation

- [1] a) S. Anderson, H. L. Anderson, J. K. M. Sanders, *Acc. Chem. Res.* **1993**, *26*, 469; b) D. Holtz, D. F. Bocian, J. S. Lindsey, *Acc. Chem. Res.* **2002**, *35*, 57; c) Y. Nakamura, N. Aratani, A. Osuka, *Chem. Soc. Rev.* **2007**, *36*, 831; d) N. Aratani, D. Kim, A. Osuka, *Acc. Chem. Res.* **2009**, *42*, 1922.
- [2] a) K. Sugiura, Y. Fujimoto, Y. Sakata, *Chem. Commun.* **2000**, 1105; b) A. Kato, K. Sugiura, H. Miyasaka, H. Tanaka, T. Kawai, M. Sugimoto, M. Yamashita, *Chem. Lett.* **2004**, *33*, 578; c) O. Shoji, H. Tanaka, T. Kawai, Y. Kobuke, *J. Am. Chem. Soc.* **2005**, *127*, 8599; d) J. E. Raymond, A. Bhaskar, T. D. Goodson III, N. Makiuchi, K. Ogawa, Y. Kobuke, *J. Am. Chem. Soc.* **2008**, *130*, 17212.
- [3] a) M. Hoffmann, C. J. Wilson, B. Odell, H. L. Anderson, *Angew. Chem. Int. Ed.* **2007**, *46*, 3122; *Angew. Chem.* **2007**, *119*, 3183; b) M. Hoffmann, J. Kärrbratt, M.-H. Chang, L. M. Herz, B. Albinsson, H. L. Anderson, *Angew. Chem. Int. Ed.* **2008**, *47*, 4993; *Angew. Chem.* **2008**, *120*, 5071; c) J. K. Sprafke, D. V. Kondratuk, M. Wykes, A. L. Thompson, M. Hoffmann, R. Drevinskis, W. H. Chen, C. K. Yong, J. Kärrbratt, J. E. Bullock, M. Malfois, M. R. Wasielewski, B. Albinsson, L. M. Herz, D. Zigmantas, D. Beljonne, H. L. Anderson, *J. Am. Chem. Soc.* **2011**, *133*, 17262; d) M. C. O'Sullivan, J. K. Sprafke, D. V. Kondratuk, C. Rinfrey, T. D. W. Claridge, A. Saywell, M. O. Blunt, J. N. O'Shea, P. H. Beton, M. Malfois, H. L. Anderson, *Nature* **2011**, *469*, 72.
- [4] a) X. Peng, N. Aratani, A. Takagi, T. Matsumoto, T. Kawai, I.-W. Hwang, T. K. Ahn, D. Kim, A. Osuka, *J. Am. Chem. Soc.* **2004**, *126*, 4468; b) T. Hori, N. Aratani, A. Takagi, T. Matsumoto, T. Kawai, M.-C. Yoon, Z. S. Yoon, S. Cho, D. Kim, A. Osuka, *Chem. Eur. J.* **2006**, *12*, 1319; c) T. Hori, X. Peng, N. Aratani, A. Takagi, T. Matsumoto, T. Kawai, Z. S. Yoon, M.-C. Yoon, J. Yang, D. Kim, A. Osuka, *Chem. Eur. J.* **2008**, *14*, 582; d) J. Song, S. Y. Young, S. Yamaguchi, J. Sankar, S. Hiroto, N. Aratani, J.-A. Shin, S. Easwaramoorthi, K. S. Kim, D. Kim, H. Shinokubo, A. Osuka, *Angew. Chem. Int. Ed.* **2008**, *47*, 6004; *Angew. Chem.* **2008**, *120*, 6093; e) J. Song, P. Kim, N. Aratani, D. Kim, H. Shinokubo, A. Osuka, *Chem. Eur. J.* **2010**, *16*, 3009; f) K. Osawa, J. Song, K. Furukawa, H. Shinokubo, N. Aratani, A. Osuka, *Chem. Asian J.* **2010**, *5*, 764; g) J. Song, N. Aratani, P. Kim, D. Kim, H. Shinokubo, A. Osuka, *Angew. Chem. Int. Ed.* **2010**, *49*, 3617; *Angew. Chem.* **2010**, *122*, 3699; h) J. Song, N. Aratani, H. Shinokubo, A. Osuka, *J. Am. Chem. Soc.* **2010**, *132*, 16356; i) J. Song, N. Aratani, H. Shinokubo, A. Osuka, *Chem. Eur. J.* **2010**, *16*, 13320; j) J. Song, N. Aratani, H. Shinokubo, A. Osuka, *Chem. Sci.* **2011**, *2*, 748.
- [5] a) Y. Nakamura, I.-W. Hwang, N. Aratani, T. K. Ahn, D. M. Ko, A. Takagi, T. Kawai, T. Matsumoto, D. Kim, A. Osuka, *J. Am. Chem. Soc.* **2005**, *127*, 236.
- [6] a) A. Osuka, H. Shimizu, *Angew. Chem. Int. Ed. Engl.* **1997**, *36*, 135; *Angew. Chem.* **1997**, *109*, 93; b) Y. H. Kim, D. H. Jeong, D. Kim, S. C. Jeong, H. S. Cho, S. K. Kim, N. Aratani, A. Osuka, *J. Am. Chem. Soc.* **2001**, *123*, 76; c) D. Kim, A. Osuka, *Acc. Chem. Res.* **2004**, *37*, 735.
- [7] a) H. Hata, H. Shinokubo, A. Osuka, *J. Am. Chem. Soc.* **2005**, *127*, 8264; b) H. Shinokubo, A. Osuka, *Chem. Commun.* **2009**, 1011.
- [8] J. M. Murphy, X. Liao, J. F. Hartwig, *J. Am. Chem. Soc.* **2007**, *129*, 15434.
- [9] Crystal data of **13Ni**: $C_{296}H_{328}N_{20}Ni_5$, $M_w = 4459.33$, triclinic, space group $P\bar{1}$ (No. 2), $a = 19.7258(4)$, $b = 22.9851(5)$, $c = 37.9752(8)$ Å, $\alpha = 79.6520(10)^\circ$, $\beta = 89.0890(10)^\circ$, $\gamma = 80.7140(10)^\circ$, $V = 16714.4(6)$ Å³, $Z = 2$, $D_{calc} = 0.886$ g cm⁻³, $T = 120(2)$ K, 131231 measured reflections, 49172 unique reflections, $R = 0.1079$, $R_w = 0.2761$ (all data), GOF = 1.062 ($I > 2.0\sigma(I)$). CCDC 976052 (**13**(Ni)) contains the supplementary crystallographic data for this paper. These data can be obtained free of charge from The Cambridge Crystallographic Data Centre via www.ccdc.cam.ac.uk/data_request/cif.
- [10] A. Tsuda, H. Furuta, A. Osuka, *J. Am. Chem. Soc.* **2001**, *123*, 10304.
- [11] S. Cho, M.-C. Yoon, J. M. Lim, P. Kim, N. Aratani, Y. Nakamura, T. Ikeda, A. Osuka, D. Kim, *J. Phys. Chem. B* **2009**, *113*, 10619.